Surface tension measurements of liquid pure iron and 304L stainless steel under different gas mixtures

Vincent Klapczynski, Dylan Le Maux, Mickael Courtois, Emmanuel Bertrand, Pascal Paillard

Surface tension measurements of liquid pure iron and 304L stainless steel under different gas mixtures

Vincent Klapczynski[1], Dylan Le Maux[2], Mickael Courtois[2], Emmanuel Bertrand[1] and Pascal Paillard[1]

[1] Institut des Matériaux Jean Rouxel (IMN), Université de Nantes, CNRS, Rue Christian Pauc, BP 50609, 44306 Nantes Cedex 3, France
[2] Univ. Bretagne Sud, UMR CNRS 6027, IRDL, F-56100 Lorient, France

Abstract

In this paper, the surface tension of molten pure iron and 304L stainless steel is measured under different gas mixtures (pure argon and Ar-2.5 %vol. H_2). Measurements are realized by aerodynamic levitation with an acoustic excitation. The surface tension is measured between 1756 K and 2227 K. The addition of H_2 in the surrounding gas is supposed to create a desorption of oxygen and modify surface tension. The effect of oxygen on surface tension is then analyzed.
Measurements show a linear variation of surface tension with temperature for pure iron under Ar-2.5 %vol. H_2 and a nonlinear relationship for the 304L stainless steel even when an active gas is used. This phenomenon can be explained by the short time at high temperature which does not allow oxygen desorption. Increasing the time at high temperature may change the surface tension but at the risk of evaporation of some alloy elements. The intensification of the evaporation would also disturb the surface tension measurements. In this study, the time spent at the liquid state is equivalent to that of welding and additive manufacturing processes, allowing to determine the thermocapillary coefficient (Marangoni effect) for both metals considered in these conditions. The comparison between our measurements and different data are consistent.

Keywords: surface tension, aerodynamic levitation, oscillating droplet method, stainless steel, Marangoni effect.

1. Introduction

Surface tension plays a key role in high temperature processes such as GMAW (Gas Metal Arc Welding) or WAAM (Wire Arc Additive Manufacturing). A variation of surface tension and its dependence to temperature may affect the geometry of a welding pool, which is known as Marangoni effect [1–4]. The surface tension of pure metals decreases with temperature, leading to a negative surface tension gradient ($d\gamma/dT < 0$) [5–7]. However, the presence of impurities such as oxygen or sulfur can inverse this temperature dependence and lead to a temperature domain with a positive gradient ($d\gamma/dT > 0$). This temperature range is limited and a transition to a negative gradient, such as in pure materials, is observed at high temperature. Thus, the variation of surface tension as a function of temperature leads to a "boomerang shape curve"[8]. It is shown in literature that oxygen modifies the surface tension gradient and can inverse the convection flows in liquid metals. Several models have been developed to evaluate the dependence of surface tension of liquid metals to temperature and impurities concentration such as oxygen and sulfur [9–12]. These models were developed to estimate the surface tension of a metal in presence of impurity (mainly oxygen or sulfur). Although they were developped for pure metals, they are used for couples alloy/surfactant in numerical simulation to predict liquid alloy motion in welding pool [13, 14]. A good knowledge of surface tension of metals and alloys is then necessary.

A large amount of surface tension data can be found for pure metals like iron [15], nickel [16] or titanium [10]. First measurements were performed by sessile drop method (SD). More recently, containerless techniques such as Electromagnetic Levitation (EML) were developed to avoid substrate contamination [17]. Even if this technique is accurate, the surfactant concentration cannot be easily controlled. That is why values of surface tension found in litterature are scattered for a given metal.

Only few experiments have been performed on alloys. Recently, Ozawa et al. [18], Fukuyama et al. [19] and Dubberstein et al. [20] studied the surface tension of stainless steel by EML. All of them reported that evaporation occurs during an experiment. According to Dubberstein [20], manganese evaporation in 304L steel during surface tension measurement leads to an overestimation the surface tension. As a pure metal, this element has a lower surface tension than other alloying elements and its presence as alloying elements should lower the surface tension value. A short time at high temperature should be imposed to perform an accurate measurement.

The aim of this work is to measure the surface tension of pure iron and 304L stainless steel by aerodynamic levitation under two gas mixtures: pure argon and argon with 2.5 %vol. H_2. Dihydrogen is mixed with argon in order to remove traces of oxygen and sulfur at the surface of the liquid metal. Firstly, pure iron is characterized under Ar-2.5 %vol. H_2 in order to confirm the validity of the measurement technique. Then, 304L is characterized under pure argon and Ar-2.5 %vol. H_2 in order to highlight the effect of oxygen under these conditions. The effect of oxygen on surface tension is estimated, discussed and compared with data of literature. The role of the experimental parameters (measurement technique and parameters) is also discussed.

2. Materials and methods

99.95 % pure iron (supplier: Neyco) and 304L stainless steel (supplier: QUADA V+F) are characterized in this experience. The composition of 304L stainless steel studied is given in Table 1.

Cr	Ni	Mn	Si	Cu	Mo	S	O
19.24	7.93	1.83	0.39	1.21	0.22	0.008	0.0083

Table 1. Chemical composition (mass %) of a SUS 304L.

45 mg samples are cut from a bulk material. They are melted under controlled atmosphere in the levitation device in order to obtain a sphere shaped sample. Then, a flat area is grinded with SiC papers in order to stabilize the levitation and avoid the rotation of the sample, as shown on Fig. 1.

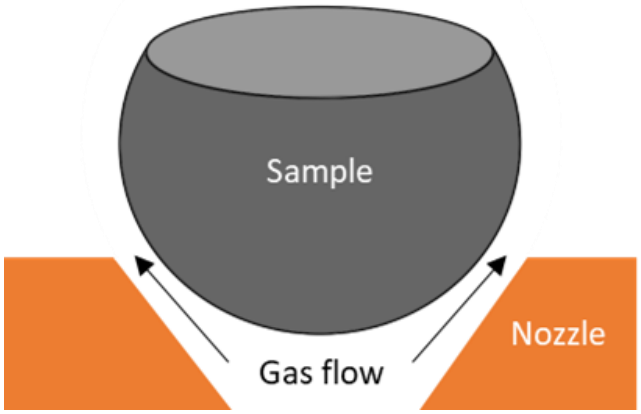

Fig. 1. Scheme of a sample before a measurement.

The mass of the sample is measured with a precision scale (Mettler Toledo XS205DU). The loss of mass due to evaporation is obtained by comparison of the mass of the sample before and after the levitation experience. A scanning electron microscope (Zeiss MERLIN) associated with an Energy Dispersive Spectrometer (Oxford instruments plc) is used to perform chemical analysis.

Surface tension measurements were performed by aerodynamic levitation on a device developed at IRDL - CNRS Laboratory. Details about the levitation technique and the experimental procedure of this study are available in a previously published work [21]. The experiment consists in putting a sample in levitation by using a numerically controlled gas flow (Brooks SLA5800) at 2.4 L min^{-1}. The chamber is purged twice before the levitation with a primary vacuum pump and filled with the required gas. This procedure ensured a low residual oxygen content (below 5 ppm when using argon). Once in levitation, the sample is heated until melting with a 300 W diode laser (IPG YLR 300/3000 QCW λ = 1070 nm). The laser sequence is constituted of a very short time with a high power in order to melt the sample quickly (1.5 s at 140 W) and a power stabilization stage (for example 5.5 s at 30 W) in order to reach several temperature range, see Fig. 2. Temperature of the sample is measured using a bichromatic pyrometer (Optris CT Ratio 2MH1). The emissivity ratio is calibrated by measuring the solidification temperature of pure iron which occurs at 1811 K.

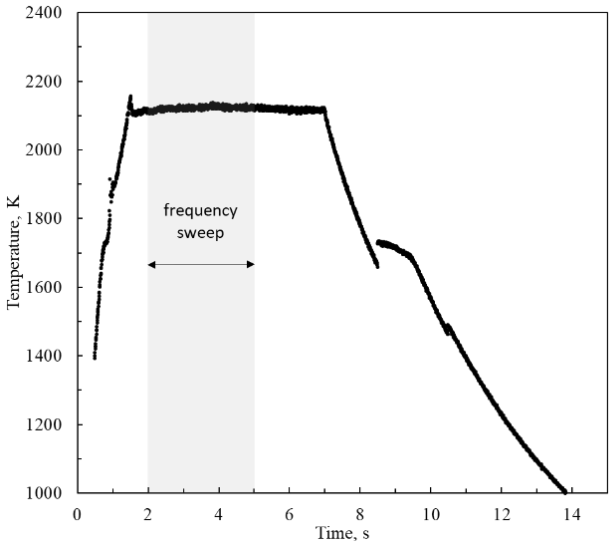

Fig. 2. Standard temperature measurement on a sample.

A high-speed camera (Phantom VEO-E 310L) is employed at 2000 fps to record oscillation movements during the acoustic excitation. The acoustic excitation is realized by a loudspeaker positioned in the vacuum chamber. The acoustic

wave is guided under the sample and consists in a frequency sweep between 160 Hz and 220 Hz for a duration of 3 s, see Fig. 3.

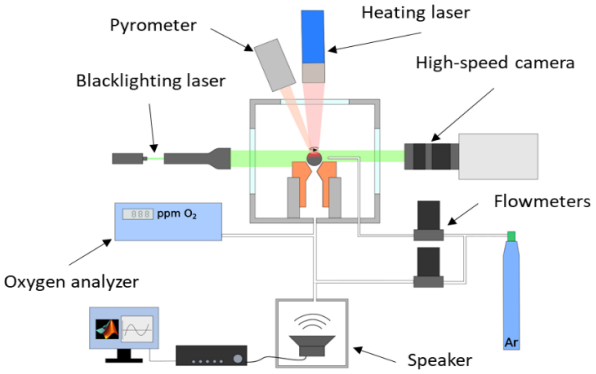

Fig. 3. Scheme of levitation device.

A Matlab program is developped to analyze the record. The amplitude of the sample oscillations is analyzed and a Fast Fourier Transform (FFT) is calculated, see Fig. 4. The spectrum allows to estimate the Rayleigh frequency ν_r, for the n=2 mode and then to calculate the surface tension, using Eq. 1 [22–24].

$$\gamma = \frac{3}{8}\pi m \nu_r^2 \quad \text{Eq. (1)}$$

However, the spectrum reveals three frequencies peaks in most of the experiences, or five peaks in some cases see Fig. 4. These peaks correspond to the ± 2 and ± 1 degenerated modes [25]. Actual experimental setup does not allow to index these peaks. Because there is a small error and it's easier to measure, only three peaks are used to calculate the Rayleigh frequency when they are observed, as suggested by Millot et al. [26].

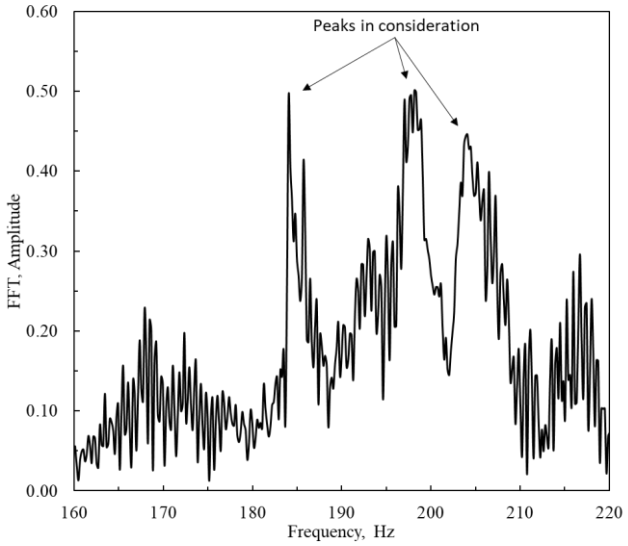

Fig. 4. Example of a Fast Fourrier Transform (amplitude normalized to 1).

3. Results and discussion

3.1 Surface tension of pure iron under Ar-2.5 %vol. H_2

Firstly, the surface tension of pure iron is measured in a range of 368 K (1859 K – 2227 K). These results are compared to experiments of literature on Fig. 5 and summarized on Table 2. Measures are in agreement with literature and a linear dependence to temperature is observed. The surface tension gradient is estimated to -1.54×10^{-4} N m^{-1} K^{-1} and the temperature dependence can be approximated by:

$$\gamma = -1.54\,.\,10^{-4}(T - 1811.15) + 1.86\ N\ m^{-1}$$

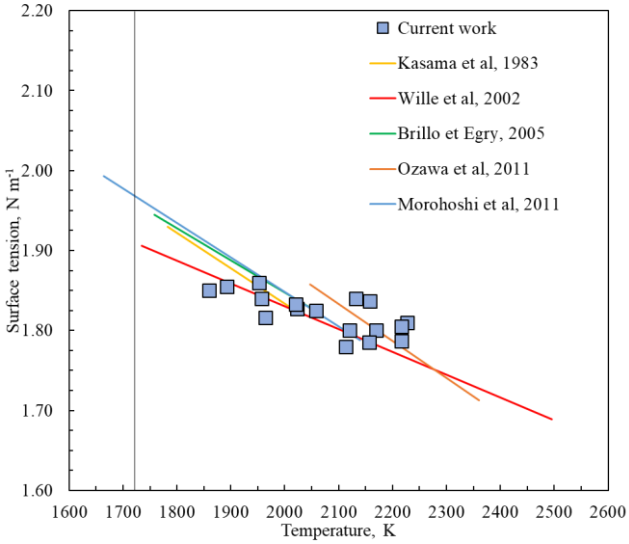

Fig. 5. Surface tension of pure 99.95 % iron under Ar-2.5 %vol. H_2 and data from literature.

γ_{1811} (N m^{-1})	dγ/dT (10^{-4} N m^{-1} K^{-1})	Temperature (K)	Purity (%)	Method	Reference
1.862	-1.54	1 859 – 2 227	99.95	ADL	Current work
1.969	-4.65	2 047 – 2 360	/	EML	(Ozawa et al., 2011) [6]
1.87	-4.30	1 750 – 1 925	/	EML	(K.C Mills and Brooks, 1994) [27]
1.92	-3.97	1 758 – 2 064	/	EML	(J. Brillo and Egry, 2005) [16]
1.925	-4.55	1 664 – 2 140	99.997	EML	(Morohoshi et al., 2011) [15]
1.888	-2.85	1 735 – 2 500	99.99	ADL	(Wille, Millot, and Rifflet, 2002) [28]
1.918	-4.30	1 781 – 2 015	99.99	EML	(Kasama et al., 1983) [29]

Table 2. Surface tension data for pure iron measured by Aerodynamic Levitation and by Electromagnetic Levitation.

As shown in table 2, the absolute value of the surface tension gradient is lower than the data from literature. However, the only measure of surface tension of pure iron by ADL [28] also highlights a higher surface tension gradient. Wille et al. only estimate a value lower than 4×10^{-4} N m^{-1} K^{-1}, see Table 2. They performed a measurement up to 2500 K, which is the highest temperature found in literature. This comparison indicates a good agreement even if no mathematical correction is employed in ADL.

3.2 Evaporation during a surface tension measurement

Several alloying elements, such as manganese and copper are known to evaporate in molten 304L [30, 31]. Preliminary tests were performed to study the impact of manganese evaporation. This experiment consists in heating several samples with different laser sequences. After the test, the loss of mass is controlled and the variation of samples composition is analyzed by Energy-Dispersive X-ray Spectroscopy (EDS).

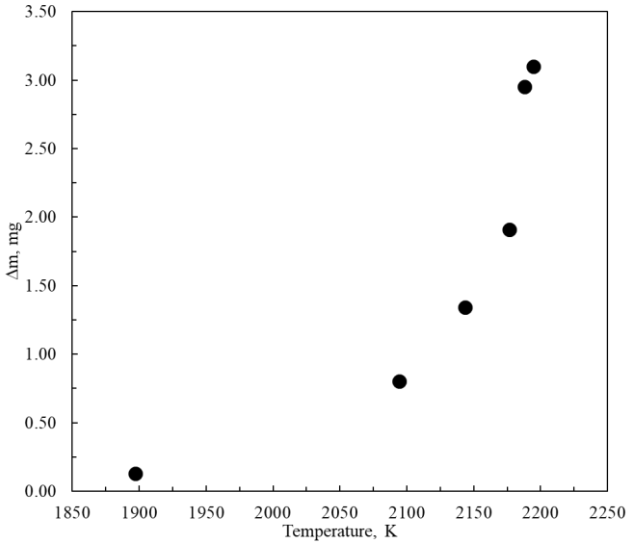

Fig. 6. Sample loss of mass as a function of temperature - dwell time of 7.5 s.

An exponential dependence between the loss of mass and temperature is evidenced, see Fig. 6. At 1997 K, the loss mass is of 0.33 %. This value increases up to 7.37 % at 2194 K. An EDS analysis, is performed to identify and quantify the evaporation of our alloy elements, as visible on table 3. Measurements show that manganese evaporation is mainly responsible of the loss of mass, followed by copper and chromium.

The impact of this phenomenon can be observed during the recording of the oscillating droplet, see Fig 7. Metallic vapor can be observed above the droplet. In order to reduce at maximum this phenomena, the dwell time at high temperature is limited to 6 seconds, the loss of mass is limited to a maximum of 3 % with these conditions.

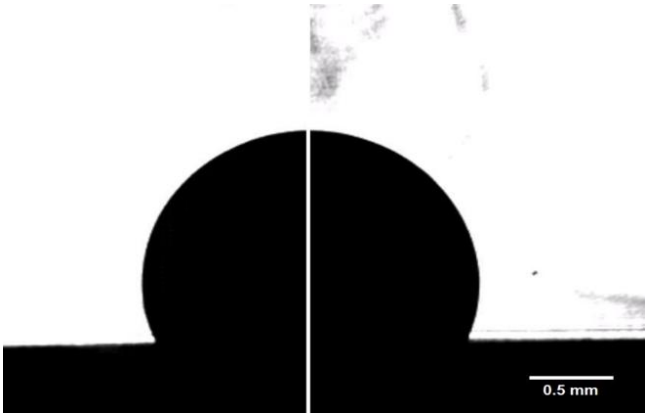

Fig. 7. Photography of a sample without metallic vapor (left) and surrounded by metallic vapor (right).

3.3 Surface tension of 304L stainless steel under 100 % Ar

The surface tension is measured in a range of 325 K (1815 K – 2140 K). These results are visible on Fig. 8. The behavior of surface tension with temperature can be split into two parts: the first domain shows an increase of surface tension with temperature and then a decrease of the surface tension with temperature, which is characteristic of a metal with impurities. In this case, samples have naturally few ppm of sulfur and oxygen. This presence, in very low quantity, is sufficient to modify the surface tension gradient. The inflection point is located around 1980 K. It is difficult to measure at high temperature the surface tension. This is due to the higher evaporation rate which disturbs flows and levitation stability. This may lead to disrupt the calculation of ν_r and then the calculation of surface tension.

Laser power (W)	Δm (mg)	Loss (%)	Temperature (K)	Mn (W %)	Cu (W %)	Cr (W %)
0*	/	/	/	1.83	1.21	19.24
20	0.13	0.33	1897	1.46	1.11	19.13
30	0.80	2.33	2094	0.51	0.78	19.21
50	1.34	2.82	2144	0.58	0.82	19.34
70	1.91	5.15	2177	0.16	0.46	19.01
90	3.10	8.13	2195	0.15	0.32	18.20
100	2.95	7.37	2188	0.26	0.15	18.38

Table 3. Estimation of the loss of mass for manganese, copper and chromium by EDS. * Initial composition as reference.

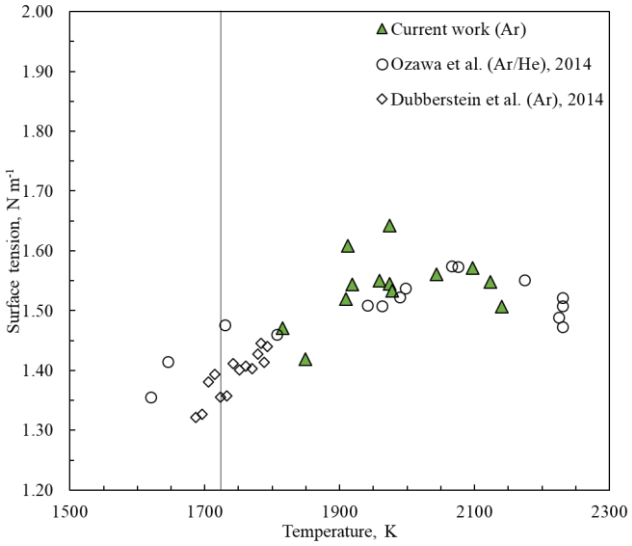

Fig. 8. Surface tension of molten 304L under 100 % Ar, comparison with Ozawa [18] and Dubberstein [20].

The surface tension temperature dependence can be approximately expressed by two equations:

$$\gamma = 7.95\,.\,10^{-4}(T - 1723.15) + 1.38\ N\ m^{-1}$$
$$T\ \in [1815\,;1975]\ K$$

$$\gamma = -3.61\,.\,10^{-4}(T - 1723.15) + 1.68\ N\ m^{-1}$$
$$T\ \in [1975\,;2140]\ K$$

The surface tension gradient is first positive with a value of 7.95 × 10^{-4} N m^{-1} K^{-1} and at around 1975 K the sign changes with a value of -3.61 × 10^{-4} N m^{-1} K^{-1}. These results are in good agreement with Ozawa's and Dubberstein's measurements [18, 20]. Moreover, no clear variation can be observed by comparing all data. Despite the presence of few ppm of surfactants (oxygen and sulfur) and the variation of manganese concentration, see Table 4. The manganese evaporation has no obsverbable effect on the surface tension value between these expirements. Nevertheless, the comparison seems pertinent and it allows to confirm a tendency.

Reference	Mn (W%)	S (ppm)	O (ppm)
Ozawa [18]	< 0.01	< 10	/
Dubberstein [20]	1.38	125	55
This paper	1.84	80	83

Table 4. Manganese, sulfur and oxygen content before trials.

3.4 Surface tension of a 304L stainless steel under Ar-2.5 %vol. H_2

During the experiment, the oxygen content in the gas cannot be measured because the sensor can be damaged in presence of hydrogen. Yet, with this gas mixture, the probable oxygen concentration is maintained to a very low value due to the hydrogen/oxygen reaction. The surface tension is measured in a range of 324 K (1756 K – 2080 K). Measurements are shown in Fig. 9.

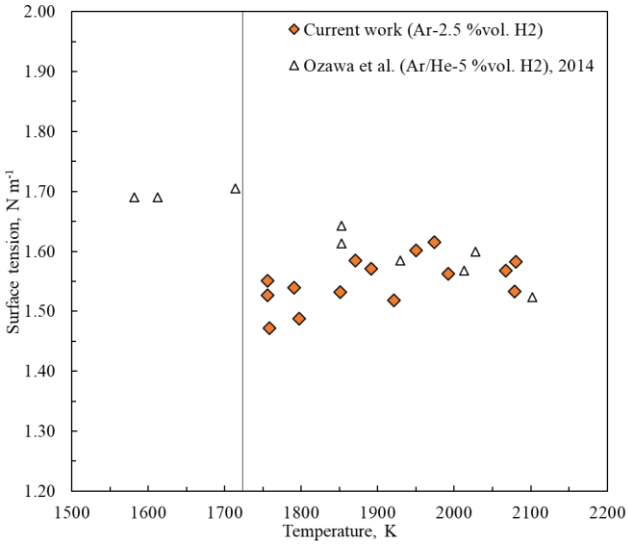

Fig. 9. Surface tension of molten 304L under Ar-2.5 %vol. H_2, comparison with Ozawa [18].

The surface tension can be approximated by using these two equations:

$$\gamma = 3.65\,.\,10^{-4}(T - 1723.15) + 1.50\ N\ m^{-1}$$
$$T\ \in [1756\,;1975]\ K$$

$$\gamma = -3.43\,.\,10^{-4}(T - 1723.15) + \ 1.68\ N\ m^{-1}$$
$$T\ \in [1975\,;2080]\ K$$

No clear difference can be observed with the measurements done under argon. A boomerang shape curve is also observed. The surface tension increases up to 1975 K with a coefficient of 3.65×10^{-4} N m^{-1} K^{-1} and then decreases slightly with a value of -3.43×10^{-4} N m^{-1} K^{-1}.

This unexpected result can be explained by experimental conditions. In order to limit the loss of mass and the modification of chemical composition, the duration above the liquidus is limited at ≈ 6 s. This duration is too short to let the desoxidation of 304L by hydrogen. Thus, experimental conditions should limit the oxygen desorption.

With these measurements, a longer dwell time at high temperature under Ar-2,5 %vol. H_2 must lead to the results of Ozawa et al. [18]. However, carrying a longer experiment would lead to the evaporation of manganese and other elements of the alloy giving results not transposable to welding and additive manufacturing processes. This can be a problem when an alloy with a high content of manganese is characterized.

3.5 Comparison between argon and Ar-2.5 %vol. H_2 measurements

The comparison of these two experiments highlights small differences. Higher values are observed in a range of 1723 K – 1970 K under Ar-2.5 %vol. H_2. In addition, surface tension values seem to be similar above 1975 K, see Fig. 10.

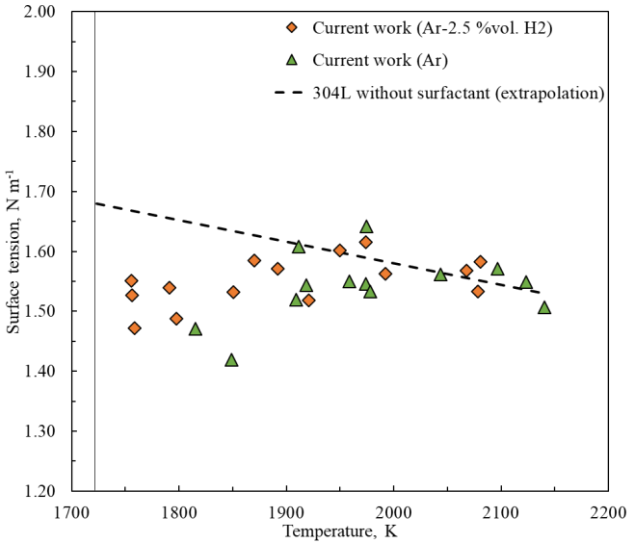

Fig. 10. Surface tension of molten 304L under Ar and Ar-2.5 %vol. H_2.

This difference can be caused by a small oxygen desorption even if the melting time is short. The oxygen concentration at the surface may be lower in presence of Ar-2.5 %vol. H_2 gas. Then, the surface tension values slightly increase below 1975 K under Ar-2.5 %vol. H_2. Beyond this temperature, no difference can be observed between these two experiments. In this temperature range, the values are equivalent to the surface tension of 304L without surfactant. The pure state value can be approximated by this equation:

$$\gamma = -3.52\ 10^{-4}(T - 1723.15) + 1.68\ N\ m^{-1}$$

This equation is in agreement with the value given by Ozawa et al. [18] with a gradient of -3.29 × 10^{-4} N m^{-1} K^{-1}. Also, it is interesting to notice that the surface tension gradient for pure liquid iron is close from this value, see Table 2. The value given in this paper is the highest. This may be the result of the iron purity used (99.95 %).

Conclusion

An aerodynamic experimental set up is used to measure the surface tension of pure liquid iron and 304L stainless steel. The temperature range is of 368 K (1859 K – 2227 K) for pure iron.

For pure iron, measurements were performed under a mixture of Ar-2.5 %vol. H_2. The variation of surface tension is in agreement with literature and validates the procedure.

For the stainless steel, surface tension was measured under two gas mixtures. The first plotted measurements under argon, presents a "boomerang shape". The curve is in good agreement with Ozawa's data with the same variation. Dubberstein does not observe a "boomerang shape". This can be explained by the shorter temperature range in his work. However, the surface tension in this temperature range is consistent.

The second curve under Ar-2.5 %vol. H_2 shows a "boomerang shape". This variation can be explained by the short time above the melting point. This dwell time does not allow long time reaction between oxygen and hydrogen. Thus oxygen desorption does not clearly appear. Longer dwell time at high temperature may affect the chemical composition of the alloy and thus modify the value. Yet, the surface tension measured may not be representative in the case of a 304L stainless steel with a higher manganese content. Results proposed here are the closest to welding and additive manufacting processes.

All these results indicate that this step up allows to measure precisely the surface tension by aerodynamic levitation up to 2227 K.

References

[1] S. Lu, H. Fujii, K. Nogi, Marangoni convection and weld shape variations in He–CO2 shielded gas tungsten arc welding on SUS304 stainless steel, J Mater Sci. 43 (2008) 4583–4591. https://doi.org/10.1007/s10853-008-2681-3.

[2] P. Rajesh Kannan, V. Muthupandi, K. Devakumaran, On the effect of temperature coefficient of surface tension on shape and geometry of weld beads in hot wire gas tungsten arc welding process, Materials Today: Proceedings. 5 (2018) 7845–7852. https://doi.org/10.1016/j.matpr.2017.11.465.

[3] A. Berthier, Analyse des phénomènes de transfert et couplages physico-chimiques lors de la transformation des métaux sous arc électrique, 2009.

[4] S. Lu, H. Fujii, H. Sugiyama, M. Tanaka, K. Nogi, Effects of Oxygen Additions to Argon Shielding Gas on GTA Weld Shape, ISIJ International. 43 (2003) 1590–1595. https://doi.org/10.2355/isijinternational.43.1590.

[5] I. Egry, E. Ricci, R. Novakovic, S. Ozawa, Surface tension of liquid metals and alloys — Recent developments, Advances in Colloid and Interface Science. 159 (2010) 198–212. https://doi.org/10.1016/j.cis.2010.06.009.

[6] S. Ozawa, S. Suzuki, T. Hibiya, H. Fukuyama, Influence of oxygen partial pressure on surface tension and its temperature coefficient of molten iron, Journal of Applied Physics. 109 (2011) 014902. https://doi.org/10.1063/1.3527917.

[7] K.C. Mills, Y.C. Su, Review of surface tension data for metallic elements and alloys: Part 1 – Pure metals, International Materials Reviews. 51 (2006) 329–351. https://doi.org/10.1179/174328006X102510.

[8] S. Ozawa, M. Nishimura, K. Kuribayashi, Surface Tension of Molten Silver in Consideration of Oxygen Adsorption Measured by Electromagnetic Levitation, International Journal of Thermophysics. (2016) 6. https://doi.org/10.1007/s10765-014-1674-5.

[9] P. Sahoo, T. Debroy, M.J. McNallan, Surface Tension of Binary Metal - Surface Active Solute Systems under Conditions Relevant to Welding Metallurgy, Metallurgical Transactions B. 19B (1988) 483–491. https://doi.org/10.1007/BF02657748.

[10] J. Brillo, J. Wessing, H. Kobatake, H. Fukuyama, Surface tension of liquid Ti with adsorbed oxygen and its prediction, Journal of Molecular Liquids. 290 (2019) 111226. https://doi.org/10.1016/j.molliq.2019.111226.

[11] A.E. Gheribi, M. Vermot des Roches, P. Chartrand, Modelling the surface tension of liquid metals as a function of oxygen content, Journal of Non-Crystalline Solids. 505 (2019) 154–161. https://doi.org/10.1016/j.jnoncrysol.2018.10.006.

[12] A.E. Gheribi, P. Chartrand, Temperature and oxygen adsorption coupling effects upon the surface tension of liquid metals, Sci Rep. 9 (2019) 7113. https://doi.org/10.1038/s41598-019-43500-3.

[13] W. Dong, S. Lu, D. Li, Y. Li, Modeling of the Weld Shape Development During the Autogenous Welding Process by Coupling Welding Arc with Weld Pool, J. of Materi Eng and Perform. 19 (2010) 942–950. https://doi.org/10.1007/s11665-009-9570-z.

[14] Y. Wang, H.L. Tsai, Effects of surface active elements on weld pool fluid flow and weld penetration in gas metal arc welding, Metall and Materi Trans B. 32 (2001) 501–515. https://doi.org/10.1007/s11663-001-0035-5.

[15] K. Morohoshi, M. Uchikoshi, M. Isshiki, H. Fukuyama, Surface Tension of Liquid Iron as Functions of Oxygen Activity and Temperature, ISIJ Int. 51 (2011) 1580–1586. https://doi.org/10.2355/isijinternational.51.1580.

[16] J. Brillo, I. Egry, Surface tension of nickel, copper, iron and their binary alloys, J Mater Sci. 40 (2005) 2213–2216. https://doi.org/10.1007/s10853-005-1935-6.

[17] I. Egry, I. Ricci, R. Novakovic, S. Ozawa, Surface tension of liquid metals and alloys - Recent developments, Elsevier. (2010). https://doi.org/10.1016/j.cis.2010.06.009.

[18] S. Ozawa, K. Morohoshi, T. Hibiya, Influence of Oxygen Partial Pressure on Surface Tension of Molten Type 304 and 316 Stainless Steels Measured by Oscillating Droplet Method Using Electromagnetic Levitation, ISIJ Int. 54 (2014) 2097–2103. https://doi.org/10.2355/isijinternational.54.2097.

[19] H. Fukuyama, H. Higashi, H. Yamano, Thermophysical Properties of Molten Stainless Steel Containing 5 mass % B_4C, Nuclear Technology. 205 (2019) 1154–1163. https://doi.org/10.1080/00295450.2019.1578572.

[20] T. Dubberstein, H.-P. Heller, J. Klostermann, R. Schwarze, J. Brillo, Surface tension and density data for Fe–Cr–Mo, Fe–Cr–Ni, and Fe–Cr–Mn–Ni steels, J Mater Sci. 50 (2015) 7227–7237. https://doi.org/10.1007/s10853-015-9277-5.

[21] D. Le Maux, M. Courtois, T. Pierre, B. Lamien, P. Le Masson, Density measurement of liquid 22MnB5 by aerodynamic levitation, Review of Scientific Instruments. 90 (2019) 074904. https://doi.org/10.1063/1.5089620.

[22] R.F. Brooks, A.P. Day, Observation of the Effects of Oxide Skins on the Oscillations of Electromagnetically Levited Metal Droplets, International Journal of Thermophysics. 20 (1999) 1041–1050. https://doi.org/10.1023/A:1022642501415.

[23] M.P. SanSoucie, J.R. Rogers, V. Kumar, J. Rodriguez, X. Xiao, D.M. Matson, Effects of Environmental Oxygen Content and Dissolved Oxygen on the Surface Tension and Viscosity of Liquid Nickel, Int J Thermophys. 37 (2016) 76. https://doi.org/10.1007/s10765-016-2085-6.

[24] I. Seyhan, I. Egry, The Surface Tension of Undercolled Binary Iron and Nickel Alloys and the Effect of Oxygen on the Surface Tension of Fe and Ni, International Journal of Thermophysics. 20 (1999) 1017–1028. https://doi.org/0195-928X/99/0700-1017116.00/0.

[25] D.L. Cummings, D.A. Blackburn, Oscillations of magnetically levitated aspherical droplets, J. Fluid Mech. 224 (1991) 395–416. https://doi.org/10.1017/S0022112091001817.

[26] F. Millot, J.C. Rifflet, V. Sarou-Kanian, G. Wille, High-Temperature Properties of Liquid Boron from Contactless Techniques, International Journal of Thermophysics. 23 (n.d.). https://doi.org/10.1023/A:1019836102776.

[27] K.C. Mills, R.F. Brooks, Measurements of thermophysical properties in high temperature melts, Materials Science and Engineering: A. 178 (1994) 77–81. https://doi.org/10.1016/0921-5093(94)90522-3.

[28] G. Wille, F. Millot, J.C. Rifflet, Thermophysical Properties of Containerless Liquid Iron up to 2500 K, International Journal of Thermophysics. 23 (2002). https://doi.org/10.1023/A:1019888119614.

[29] A. Kasama, A. McLean, W.A. Miller, Z. Morita, M.J. Ward, Surface Tension of Liquid Iron and Iron-Oxygen Alloys, Canadian Metallurgical Quarterly. 22 (1983) 9–17. https://doi.org/10.1179/cmq.1983.22.1.9.

[30] J.P. Bellot, H. Duval, M. Ritchie, A. Mitchell, D. Ablitzer, Evaporation of Fe and Cr from Induction-stirred Austenitic Stainless Steel. Influence of the Inert Gas Pressure., ISIJ International. 41 (2001) 696–705. https://doi.org/10.2355/isijinternational.41.696.
[31] M.M. Collur, A. Paul, T. Debroy, Mechanism of alloying element vaporization during laser welding, MTB. 18 (1987) 733–740. https://doi.org/10.1007/BF02672891.